

# COMPREHENSIVE STUDY OF CHROMIUM HEAVY METAL ADSORPTION FROM TEXTILE WASTEWATER USING NATURAL COMPOSITE ADSORBENT

A.A.B. Haryanto<sup>1</sup>, A.H. Ramelan<sup>2</sup>, M.Th.S. Budiastuti<sup>3</sup> and Pranoto<sup>4,✉</sup>

<sup>1</sup>Doctoral Program of Environmental Sciences, Universitas Sebelas Maret, Surakarta-57126, Indonesia

<sup>2</sup>Department of Physics, Universitas Sebelas Maret, Surakarta-57126, Indonesia

<sup>3</sup>Department of Environmental Science, Universitas Sebelas Maret, Surakarta-57126, Indonesia

<sup>4</sup>Department of Chemistry, Universitas Sebelas Maret, Surakarta-57126, Indonesia

✉Corresponding Author: pakpranotomipa@staff.uns.ac.id

## ABSTRACT

In this work, the utilization of natural composite adsorbent for the adsorption of chromium heavy metal in textile effluent has been investigated. This research aims to study the chemical and physical characteristics of natural composite Andisol-Zeolite-Fly Ash-Activated Carbon (AZFC) on the potential adsorption of chromium ions. This study performed the characterization analysis through Fourier Transform Infrared (FTIR), X-Ray Diffraction (XRD), Surface Area Analyzer (SAA), Atomic Absorption Spectrometry (AAS), and Ultraviolet-Visible Spectrometry (UV-Vis). The optimum composition of AZFC was obtained in the andisol/zeolite/activated carbon/fly ash soil ratio is 40/40/10/10, respectively. After the adsorbent was activated, the natural composite with the various ratios have been tested with the initial standard solution of 50 ppm chromium, and the adsorption process showed 99% chromium removal ion is achievable. Further, while using the actual industrial textile wastewater containing 0.15 ppm chromium, the concentration of chromium decreased by more than 82%.

**Keywords:** Adsorption, Textile Wastewater, Composite, Chromium.

RASĀYAN *J. Chem.*, Vol. 15, No.4, 2022

## INTRODUCTION

The textile industry has been prioritized for national development due to its important role in the national economy as a contributor to foreign exchange. Besides, the textile industry is also an industry that is relied on to meet the requirements of national clothing. However, the textile industry has an unfavorable environmental impact. Textile waste is the dominant wastewater produced by the textile industry due to the dyeing process. Apart from containing dyes, textile waste also contains several heavy metals.<sup>1</sup> Heavy metals are well-known as environmental polluting agents. Thus, waste containing heavy metals needs to be managed properly before being disposed of in the environment. Heavy metal is difficult to degrade by nature as it is one of the toxic pollutants.<sup>2</sup> The source of liquid waste in the textile industry comes from finishing, dyeing, printing, and wastewater treatment plants (WWTP). Based on the Minister of Environment and Forestry Regulation no. 5 of 2014, the main cause of pollution by textile factories is in the form of heavy metals, especially metal elements such as As, Pb, Cu, Cd, Cr, Zn, and halogenated hydrocarbons derived from the cleaning and finishing process. One of the heavy metal components in textile wastewater is Cr metal. If the wastewater contains Cr metal directly disposed of without proper treatment, it can endanger the environment and the surrounding community.<sup>3</sup> Textile waste treatment processes include coagulation-flocculation<sup>4</sup>, ion exchange<sup>5</sup>, filtration<sup>6</sup>, reverse osmosis<sup>7</sup>, and adsorption.<sup>8</sup> Adsorption is a process that has high effectiveness and is relatively cheaper than other processes. The development of natural materials as raw materials for adsorbents has been developed recently. For example, natural materials that have potential as an adsorbent base material such as andisol soil<sup>9</sup>, zeolite<sup>10</sup>, and activated carbon derived from coconut shells.<sup>11</sup> On the other hand, fly ash is a waste compound but can be used as an adsorbent.<sup>12</sup> The adsorption ability of any material is influenced by its surface area, pore size, and pore distribution.<sup>13</sup>

This study aims to evaluate the effectiveness of andisol soil, zeolite, activated carbon, and fly ash as the composite base material in a comprehensive trapping application for textile wastewater treatment, especially Cr.

## EXPERIMENTAL

The main materials in this study were andisol soil taken from Mount Lawu, activated carbon (bratachem, Indonesia), fly ash, and Indonesia's natural zeolite. All of the materials were prepared and characterized by mortar, sieving machine, furnace (Nabertherm), XRD (Bruker D2 phase 2<sup>nd</sup> Gen), UV-VIS (Hitachi), and FTIR (Shimadzu IR Prestige 21). Zeolite and andisol soil were washed using distilled water and then dried at room temperature. Afterward, the andisol and zeolite soil were dried at 105 °C for 5 hours<sup>14</sup> and then mashed and filtered to pass a 150 mesh sieve. 50 g of andisol and zeolite powder, respectively, were then activated by adding 250 mL of 3M NaOH solution, then stirred and heated at 70 °C for 2 hours. In the following preparation, andisol and zeolite were neutralized using distilled water and then dried. Activated carbon and fly ash dried at 60 °C for 3 hours. After that, mashed and filtered to pass a 150-mesh sieve. The previously prepared materials (andisol soil, natural zeolite, activated carbon, and fly ash) mixed with a ratio (g/g) of 40:40:10:10; 40:40:5:15; 40:40:15:5 respectively. The constant comparison of andisol and zeolite soil refers to research conducted by Pranoto *et al.* 2017.<sup>8</sup> 10 g of the composite was added into 50mL of 50 ppm Cr (VI) standard solution for 2 hours with a constant shake. The decrease in Cr (VI) concentration was then calculated using an AAS spectrophotometer. The optimum composition was then tested for optimal contact time and pH variation. The contact time test was carried out by adding 0.1 g of the composite into 10 mL of Cr 2ppm standard solution with time variations (0, 15, 30, 60, 90, 120, and 150 minutes). The Cr (VI) concentration reduction was then calculated using a UV-VIS spectrophotometer measurement according to SNI (Indonesia National Standard) 6989.71: 2009. A similar procedure was done for pH variations (3, 5, 7, 9, and 11). 0.2 g of the composite was added into 10 mL of Cr solution with various concentrations of 0.1; 0.2, 0.3; 0.4; and 0.5% for two hours. The type of isotherm was determined based on the Langmuir and Freundlich equations. The composite testing on textile industry wastewater is carried out by making the composite into pellets with a diameter of 0.5 mm and a height of 10 mm. Then the pellets are put into the filtration tube and tested using wastewater from the textile industry. The results of the adsorption process were then tested based on the Regulation of Environment and Forestry Ministry No. P.16/MENLHK/SETJEN/KUM.1/4/2019 regarding wastewater quality standard.

## RESULT AND DISCUSSION

### X-Ray Diffraction Analysis

All material in this research was characterized using XRD. The diffractogram profile for each material can be seen in Fig.-1.

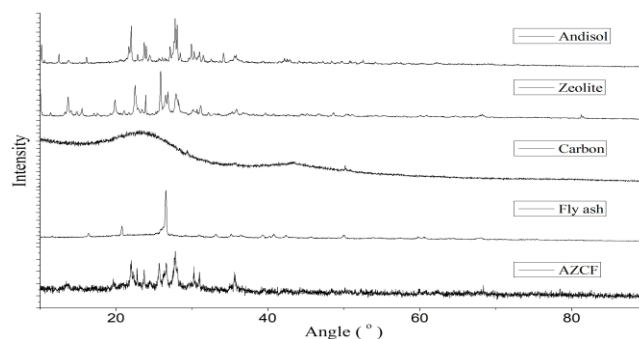


Fig.-1: Diffractogram of Materials

The calcined andisol peaks are shown at angles of 28.026° (100%), 27.78° (91.3%), 21.96° (36.6%), 30.97° (23.2%), and 23.70° (13.6%). Zeolite peaks are shown at the peaks of 26.52° (100%), 27.92° (90.3%), 22.51° (89.5%), 25.87° (75.1%), and 26.52° (72.1%). The fly ash peaks are shown at 20.78° (19%) and 26.56° (100%). The peaks of activated carbon are shown at the peaks of 23.23° and 43.22°. The zeolite has similar XRD peaks to the standard mordenite ICSD 68448 and Clinoptilolite ICSD

66457.<sup>10-15</sup> Meanwhile, fly ash is similar to the XRD peak with quartz ICSD 173227 and Mullite ICSD 23867 standards. It shows the dominant result on the XRD diffractogram is the quartz phase ( $\text{SiO}_2$ ). Composite has XRD peaks similar to the XRD peaks of zeolite, andisol, and fly ash. Activated carbon has amorphous peaks and widened so that the XRD peaks of activated carbon on composites are not visible. Composite XRD peaks are shown at angles of  $21.99^\circ$  (84.3%),  $22.75^\circ$  (69.7%),  $23.69^\circ$  (67.4%),  $25.7^\circ$  (79.2%),  $26.3^\circ$  (65.9%),  $26.66^\circ$  (76.8%),  $27.80^\circ$  (100%), and  $30.22^\circ$  (72.5%). From those results, it can be said that the composite is composed of andisol, zeolite, fly ash, and activated carbon.

### Fourier Transform Infrared Analysis

The natural andisol spectra in Fig.-2 show the absorption at 3400, 1700, 970, 650, and 450  $\text{cm}^{-1}$ . Khan *et al.*,<sup>16</sup> said that andisol has specific absorption in 3400, 1640, 1000, 560, 450, and 348  $\text{cm}^{-1}$ . The absorption at 3400  $\text{cm}^{-1}$  shows the vibration of  $-\text{OH}$  stretching, while the absorption at 1700  $\text{cm}^{-1}$  is the vibration of  $-\text{OH}$  bending.<sup>17</sup> Also, Putra *et al.*,<sup>15</sup> showed that the absorption at 1700  $\text{cm}^{-1}$  is also considered the  $-\text{OH}$  absorption that binds to the silanol group. The absorption at 970  $\text{cm}^{-1}$  is the vibration of  $\text{Si-O}$  stretching<sup>16</sup> and the vibrations of  $\text{Si-O-Si}$  and  $\text{Si-O-Al}$  stretching.<sup>18</sup> The absorption at 650  $\text{cm}^{-1}$  and 450  $\text{cm}^{-1}$  is in the vibration region of  $\text{O-Si-O}$  bending.<sup>16</sup> Activated andisol soil undergoes a shift in the wavenumber from the absorption area of 970  $\text{cm}^{-1}$  to 1000  $\text{cm}^{-1}$  absorption.<sup>16</sup> It indicates a  $\text{Si-O}$  tetrahedral condensation reaction followed by the breaking of the bonds in  $\text{Si-O-Al}$  linkages and dehydroxylation of the  $\text{Si-OH}$  group. The effect of wavenumber shifting can be caused by the crystal structure change of andisol to be richer in the  $\text{Si}$  content than  $\text{Al}$  in the structure.<sup>16,19</sup> Besides, there is also a widening of absorption after activation. Also, there was a decrease in the transmittance value at the absorption rate of 3500  $\text{cm}^{-1}$  and 1700  $\text{cm}^{-1}$ , which indicated a reduction of water content within the Andisol structure.

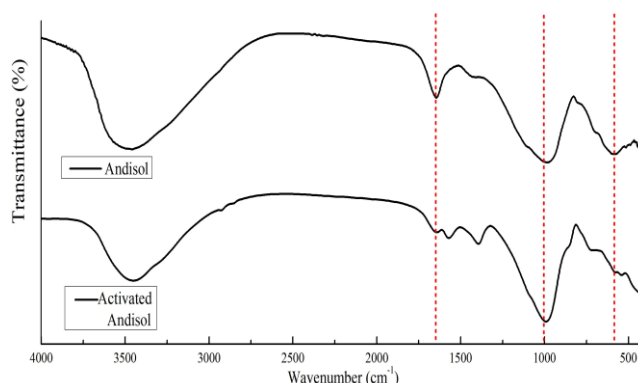


Fig.-2: FTIR Spectra of A. Andisol and B. Activated Andisol

The zeolite and fly ash show that most of them have functional groups, such as Andisols, but there are some differences, such as shifts in wavenumbers and transmittance heights. In the zeolite, the absorption of the  $-\text{OH}$  functional group shows 3 absorption peaks, namely the absorption of 3600, 3500, and 3400  $\text{cm}^{-1}$ , where the three absorption groups of  $-\text{OH}$  show as bridges (as in the  $\equiv\text{Al}(\text{OH})\text{Si}\equiv$  group with Brønsted acid character.<sup>10</sup> The absorption of  $\text{Si-O-Si}$  in the FTIR spectra aimed at 1000, 800, 650, and 400  $\text{cm}^{-1}$  wavenumbers.<sup>16,18-19</sup> Composite has FTIR peaks similar to the FTIR peaks of zeolite, andisol, and fly ash. Activated carbon has amorphous peaks and widened so that the FTIR peaks of activated carbon on composites are not visible. It is shown that the composite has an absorption at 3400  $\text{cm}^{-1}$ , which shows the vibration of  $-\text{OH}$  stretching, while the absorption at 1700  $\text{cm}^{-1}$  is the vibration of  $-\text{OH}$  bending. The absorption at 970  $\text{cm}^{-1}$  is the vibration of  $\text{Si-O}$  stretching<sup>16</sup> and the vibrations of  $\text{Si-O}(\text{Si})$  and  $\text{Si-O}(\text{Al})$  stretching. The absorption at 650  $\text{cm}^{-1}$  and 450  $\text{cm}^{-1}$  indicates the vibration region of  $\text{O-Si-O}$  bending. The process of heavy metal adsorption on the material is determined by the presence of a negatively charged functional group on its surface so that this negatively charged functional group will bind the positively charged metal. Figure-2 and Figure-3 show that andisol, zeolite, and fly ash soils have a negatively charged surface evidenced by the absorption of  $\text{Si-OH}$  and  $\text{Al-OH}$  functional groups. Those functional groups can be used to exchange cations in the absorption process of  $\text{Cr}^{6+}$  ion.<sup>14</sup>

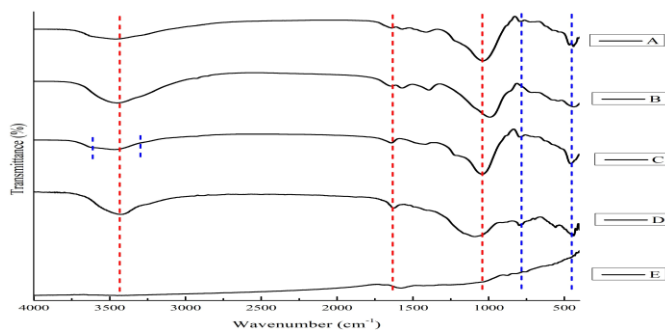


Fig.-3: FTIR spectra of A. Composite B. Activated Andisol, C. Activated Zeolite D. Fly Ash, and E. Activated Carbon

### Surface Area Analyzer Analysis

The results of the material surface analysis are shown in Table-1.

Table-1: Surface Analysis of A. Andisol, B. Activated Andisol, C. Activated Zeolite D. Fly ash and E. Activated Carbon

Material	Pore Size (Å)	Surface Area (m <sup>2</sup> /g)
Andisol	26.92	142.40
Activated Andisol	54.57	39.11
Zeolite	33.02	48.69
Activated Zeolite	81.59	18.70
Fly ash	26.36	122.70
Activated Carbon	31.44	49.60
Composite	42.97	36.21

The surface area of a material affects the adsorption capacity of the material. The surface area of andisol and zeolite decreased after the activation process. The activation process will lead to the impurity removal on the andisol soil's surface. The increase in pore size is caused by this phenomenon, where the impurities that cover the pores are destroyed after being activated using NaOH. As shown in Table-1, the material with the highest potential for adsorption is fly ash because it has a surface area of 122.7 m<sup>2</sup> g<sup>-1</sup>. Hence, the active site of fly ash is likely higher than andisol, zeolite, and activated carbon. The composite has a pore size of around 42.97 Å, and its surface area is 36.21 m<sup>2</sup>/g. The major composite composition is activated andisol and activated zeolite, affecting the decreasing composite surface area but increasing the composite pore size.

### Determination of Composite Effectiveness

This study tests the composite effectiveness by determining the optimum composition, contact time, and pH. Determination of the composite effectivity using the batch method in several variations using a standard solution of 50 ppm Cr 50 mL. The results of the uptake are shown in Table-2.

Table-2. Cr Removal by the Composites

Composite A/Z/F/C	Initial	Activated
	Removal (%)	
40/40/10/10	5.33	99.46
40/40/5/15	1.84	99.39
40/40/15/5	4.75	99.38

Table-2 shows that the activation process can increase the adsorption ability of the composites. Before being activated, the highest ability to reduce Cr metal was only 5.33%. The reduced impurity on the adsorbent surface can cause the active site of the adsorbent surface to no longer be covered.

The increase of the active site strengthens the adsorption ability of Cr metal. The three activated composites can reduce the Cr metal content above 99%. The adsorbent composition with a 40: 40: 10: 10 shows the highest adsorption ability, although the difference with other compositions is not too significant. Figure-4 shows a decrease in Cr concentration at various adsorption times. From the graph, the reduction rate of Cr concentration significantly occurred in the first 30 minutes. The longer the adsorption time, the reduction rate of Cr concentration continued to decline.

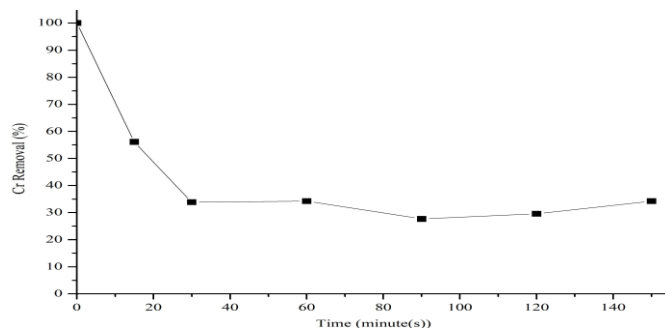


Fig.-4: Cr Removal Percentage under Various Contact Time

The adsorption process continues until 90 minutes, where at 90 minutes, there is no decrease in the concentration of Cr metal. It can be concluded that the Cr metal adsorption process reaches its highest point at 90 minutes. The adsorption process can run well in the early minutes because the adsorbent surface has not reached its saturation point. After 90 minutes of contact time, the active site of the adsorbent may have been covered by heavy metal Cr, so the rate of decline in the concentration of Cr metal did not change.

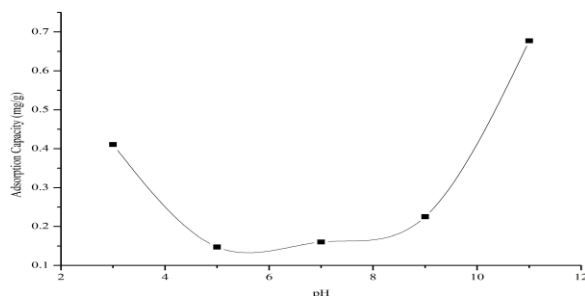


Fig.-5: Adsorption Capacity under Various pH

Figure-5 illustrates the ability of the Cr adsorption at pH variations 3, 5, 7, 9, and 11. This process is carried out to determine the adsorbent ability at certain pH conditions. It can be used to illustrate composite removal ability under real-time conditions in an environment where the pH of the wastewater will fluctuate. It can be concluded that conditions pH 3 and 11 show the highest adsorption effectiveness.

### Isotherm Adsorption Study

The isotherm adsorption type was studied to determine the physical or chemical interactions between the Cr metal and the adsorbent surface. Analyzes were performed using Langmuir (Fig.-6) and Freundlich (Fig.-7) equations.

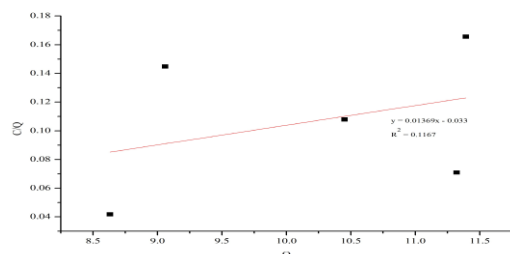


Fig.-6: Langmuir Isotherm Graph of Composite

Based on the isotherm graph, it can be concluded that the type of isotherm in this study follows the Freundlich equation with an R-square value of 0.966, while the Langmuir equation is only 0.1167. The Freundlich equation assumes that the active site molecule will bind to the adsorbate molecule with several layers (multilayer), where the particles attached to the adsorbent surface by forming van der Waals bonds, and the uptake occurs in more than one layer (multilayer).<sup>20</sup> The Freundlich isotherm system occurs in

physisorption where the bond between the Cr metal and the adsorbent surface is only weakly bonded, so the composite used is suitable for long-term use because it can be regenerated.

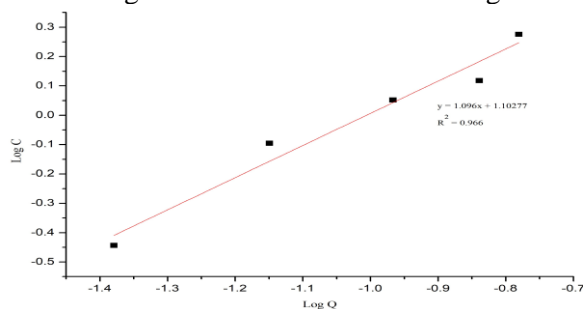


Fig.-7: Freundlich Isotherm Graph of Composite

### The Adsorption Capacity of Cr<sup>6+</sup> Ion on Textile Wastewater

The performance test of the entrapment system was carried out using textile industry wastewater that flowed through the system. The treated water is collected and measured based on the Regulation of Environment and Forestry Ministry No. P.16/MENLHK/SETJEN/KUM.1/4/2019 regarding wastewater quality standard.

The model performance test of the textile industry wastewater shows that the composite can reduce the total Cr concentration of textile industry wastewater. The wastewater has decreased in Cr concentration from 0.15 ppm to below 0.026 ppm or by more than 82%. From these results, it can be concluded that the composites used can reduce the concentration of Cr metal in the textile industry wastewater.

### CONCLUSION

XRD diffractogram shows that allophane and feldspar are the dominant andisol soil phases. Natural zeolite has a mordenite phase, fly ash contains quartz and mullite phases, and activated carbon is identified as amorphous. Furthermore, wavenumbers of negative charge functional groups such as Si-OH and Al-OH have appeared on all materials during FTIR analysis. This shows that the material can bind the Cr<sup>6+</sup> ion. The composition effectiveness analysis shows that the activation process can improve the adsorption ability in the three compositions of the materials used in the research. The decrease in the concentration of Cr metal by using a standard solution of Cr obtained a result of 99%, while the concentration of Cr metal in liquid waste decreased by more than 82%. The optimum adsorption time was obtained at 90 minutes, and the optimum pH was obtained with high effectiveness at pH 3 and 11.

### REFERENCES

1. A. Zille, *Laccase Reactions for Textile Applications*. Ph.D. Thesis, Universidade do Minho, Braga, Portugal (2005).
2. G. Zhao, X. Wu, X. Tan, and X. Wang, *The Open Colloid Science Journal*, **4**, 19(2011), <https://dx.doi.org/10.2174/1876530001104010019>
3. W. Widowati, A. Sastiono, and R. Jusuf, *Efek Toksik Logam*, Andi Offset, Yogyakarta, p.412(2008). <http://r2kn.litbang.kemkes.go.id:8080/xmlui/handle/123456789/75304>
4. S. Haydar and J. A. Aziz, *Journal of Hazardous Materials*, **168(2-3)**, 1035(2009), <https://doi.org/10.1016/j.jhazmat.2009.02.140>
5. T. Sardohan, E. Kir, A. Gulec, and Y. Cengeloglu, *Separation and Purification Technology*, **74 (1)**, 14(2010), <https://doi.org/10.1016/j.seppur.2010.05.001>
6. Y. Zhao, M. Kunieda, N. Obi, and S. Watanabe, *Precision Engineering*, **49**, 211(2017), <https://doi.org/10.1016/j.precisioneng.2017.02.009>
7. J. S. George, A. Ramos, and H. J. Shipley, *Journal of Environmental Chemical Engineering*, **3 (2)**, 969(2015), <https://doi.org/10.1016/j.jece.2015.03.011>
8. Pranoto, A. Masykur, and Y. A. Nugroho, IOP Conference Series: *Materials Science and Engineering*, **333**, 012057(2018), <http://dx.doi.org/10.1088/1757-899X/333/1/012057>

9. I. Rois, Pranoto, and Sunarto, *EnviroScienteeae*, **14(2)**, 99(2018), <https://doi.org/10.20527/es.v14i2.5475>
10. W. W. Lestari, D. N. Hasanah, R. Putra, R. R. Mukti, and K. D. Nugrahaningtyas, *IOP Conference Series: Materials Science and Engineering*, **349**, 012068(2018), <http://dx.doi.org/10.1088/1757-899X/349/1/012068>
11. M. Fadhillah and D. Wahyuni, *Jurnal Kesehatan Komunitas*, **3(2)**, 93(2016), <https://doi.org/10.25311/keskom.Vol3.Iss2.110>
12. Z. Mufrodi, N. Widiastuti, and R. C. Kardika, in *Prosiding Seminar Nasional Teknoin Bidang Teknik Kimia dan Tekstil*, B-90(2008).
13. W. Song, T. Shi, D. Yang, J. Ye, Y. Zhou, and Y. Feng, *Journal of Environmental Management*, **162(1)**, 96 (2015), <https://doi.org/10.1016/j.jenvman.2015.07.010>
14. P. Pranoto, C. Purnawan, and T. Utami, *Rasayan Journal of Chemistry*, **11(1)**, 23(2018), <http://dx.doi.org/10.7324/RJC.2018.1111939>
15. R. Putra, W. W. Lestari, F. R. Wibowo, and B. H. Susanto, *Bulletin of Chemical Reaction Engineering & Catalysis*, **13 (2)**, 245(2018), <https://doi.org/10.9767/bcrec.13.2.1382.245-255>
16. H. Khan, N. Matsue, and T. Henmi, *Clay Science*, **13(2)**, 43(2006), <https://doi.org/10.11362/jcssjclayscience1960.13.43>
17. R. Farma, D. Fatjrin, Awitdrus, and M. Deraman, *AIP Conference Proceedings*, **1801**, 040001(2017), <https://doi.org/10.1063/1.4973090>
18. M. Ristic, S. Krehula, and S. Music, *Croatica Chemica Acta*, **91(1)**, 65(2018), <https://doi.org/10.5562/cca3276>
19. Q. Xie, J. Xie, L. Chi, C. Li, D. Wu, Z. Zhang, and H. Kong, *Science China Technological Sciences*, **56 (7)**, 1749(2013), <https://doi.org/10.1007/s11431-013-5232-3>
20. M. Handayani and E. Sulistiyono, *Prosiding Seminar Nasional Sains dan Teknologi Nuklir PTNBR–BATAN Bandung*, **3**, 130(2009)

[RJC-6636/2022]